http://dx.doi.org/10.5935/0103-5053.20130110
J. Braz. Chem. Soc., Vol. 24, No. 5, 830-836, 2013.
Printed in Brazil - ©2013 Sociedade Brasileira de Química
0103 - 5053 $6.00+0.00

Article

Iron Porphyrins as Biomimetical Models for Disperse Azo Dye Oxidation

Valéria P. Barros* and Marilda D. Assis

Departamento de Química, Faculdade de Filosofia Ciências e Letras de Ribeirão Preto, Universidade de São Paulo, Av. Bandeirantes 3900, 14040-901 Ribeirão Preto-SP, Brazil

As ferroporfirinas comerciais cloreto de 5,10,15,20-*tetraquis*-(4-carboxifenil) porfirinaferro(III), cloreto de 5,10,15,20-*tetraquis*-(N-metil-4-piridil)porfirinaferro(III) e cloreto de 5,10,15,20-*tetraquis*-(2,3,4,5,6-pentafluorofenil)porfirinaferro(III) foram investigadas como modelo do citocromo P450 na oxidação dos azo corantes Disperse Black 3 (DB3), Disperse Orange 3 (DO3) e Methyl Yellow (MY). Iodosilbenzeno, *tert*-butil hidroperóxido e peróxido de hidrogênio foram utilizados como oxidantes. As reações de oxidação foram monitoradas por espectroscopia de absorção no UV-Vis em comprimento de onda característico de cada corante e identificação dos produtos por cromatografia líquida de alto rendimento (HPLC) e cromatografia gasosa-espectrometria de massas (GC-MS). Os sistemas catalíticos foram eficientes para a oxidação de todos os corantes formando os produtos 4-nitroanilina e 4,4'-dinitroazobenzeno; 4-metilamino-azobenzeno, 4-aminoazobenzeno e 4-nitroazobenzeno; e 4,4'-dinitroazobenzeno, respectivamente. Os produtos obtidos para todos os corantes são resultado da oxidação dos substituintes aminas terminais, e a ligação azo permanece intacta nestas reações para os corantes DB3 e MY. Para o corante DO3 ocorre a ruptura da ligação azo, resultando na formação da 4-nitroanilina. Produtos semelhantes são observados nos sistemas biológicos na oxidação do corante DO3, mostrando que os sistemas catalíticos estudados comportam-se como bons modelos biomiméticos.

The commercial ironporphyrins 5,10,15,20-*tetrakis*-(4-carboxyphenyl)porphyrin iron(III) chloride, 5,10,15,20-*tetrakis*-(N-methyl-4-pyridyl)porphyrin iron(III) pentachloride and 5,10,15,20-*tetrakis*-(2,3,4,5,6-pentafluorophenyl)porphyrin iron(III) chloride were investigated as cytochrome P450 models for the oxidation of the azo dyes Disperse Black 3 (DB3), Disperse Orange 3 (DO3) and Methyl Yellow (MY). Iodosylbenzene, *tert*-butyl hydroperoxide and hydrogen peroxide were used as oxidants. The oxidation reactions were monitored by UV-Vis absorption spectroscopy, by the observation of the absorption band characteristic of each dye, followed by product identification via high-performance liquid chromatography (HPLC) and gas chromatography-mass spectrometry (GC-MS). The catalytic systems were efficient for the oxidation of the dyes, leading to 4-nitroaniline and 4,4'-dinitroazobenzene; 4-methylamino-azobenzene, 4-aminoazobenzene, and 4-nitroazobenzene; and 4,4'-dinitroazobenzene as oxidation products, respectively. The oxidation products resulted from the oxidation of the terminal amine in the case of all the dyes, and the azo bond remained intact for DB3 and MY dyes. For DO3 dye, the azo bond is broken resulting in the formation of 4-nitroaniline. Similar products were observed for the oxidation of DO3 in biological systems, showing that the catalytic systems studied herein are good biomimetical models.

Keywords: disperse azo dye, metalloporphyrins, biomimetical models, oxidation, cytochrome P450

Introduction

Azo dyes represent 70% of all the dyes (10^6 tons) produced *per* year and have applications in the textile, paper, leather, gasoline, additive, foodstuff, cosmetics and pharmaceutical industries.[1-4] Some azo dyes are also used in laboratories as either biological stains or pH indicators.[1,5] Most of these synthetic dyes and their biodegradation products, sulfonated and unsulfonated aromatic amines, are toxic to aquatic organisms and suspected of being carcinogenic and mutagenic for humans.[6-9] In the mammalian liver, azo compounds are biotransformed via oxidation, conjugation hydrolysis, or reduction reactions catalyzed by enzymes, including cytochrome P450.[10-13]

*e-mail: vpbarros@yahoo.com

The superfamily of the cytochrome P450 enzymes, present in plants, bacteria and mammals, is important in the detoxification of lipophilic drugs and pollutants. They can also activate chemicals that are protoxicants and procarcinogens.[14-16] In most reactions catalyzed by cytochrome P450, one oxygen atom from a dioxygen molecule is added to a substrate (monoxygenation) via heterolysis of the O–O bond, while the other oxygen atom is reduced to water with two electrons and two protons.[17,18] These enzymes catalyze the insertion of one oxygen atom from dioxygen into many different substrates, including the epoxidation of double bonds, the oxidation of heteroatoms and the dealkylation and oxidation of aromatic carbons.[17,19] Because P450 isolation is a very delicate and expensive task, the use of P450 synthetic models can be a useful tool for xenobiotic detoxification studies. In this context, metalloporphyrins (MePs) have been widely employed as models for cytochrome P450 monooxygenase-catalyzed oxidation reactions.[15-20]

Systems containing macrocyclic compounds such as porphyrins, phthalocyanines and Schiff bases are capable of forming complexes with several transition metals with different oxidation states. These metallic compounds have the ability to mimic the catalytic behavior of peroxidase and cytochrome P450-dependent monooxygenases, both in homogeneous and heterogeneous media, for the organic substrates.[19-22] In this context, metalloporphyrins, which are capable of catalyzing redox reactions under mild conditions,[23,24] have aroused great interest for applications related to the metabolism of organic compounds such as drugs, pesticides and dyes,[19,21,24] with a view to elucidating oxidation mechanisms and developing new compounds for pharmacological and toxicological tests. Although the literature concerning dye degradation is extensive,[1,2,4,9,25] there are relatively few studies on the use of metalloporphyrins as cytochrome P450 models for dye oxidation.[20,21,26-28] Studies on metalloporphyrins can be an excellent alternative for the identification and isolation of the metabolites obtained in the *in vitro* oxidation of azo dyes, thereby aiding in the elucidation of the mechanism of these oxidations in *in vivo* systems.

In this context, in the present study the commercial ironporphyrins 5,10,15,20-*tetrakis*-(4-carboxyphenyl) porphyrin iron(III) chloride (FeTCPP) 5,10,15,20-*tetrakis*-(N-methyl-4-pyridyl)porphyrin iron(III) pentachloride (FeTMPyP) and 5,10,15,20-*tetrakis*-(2,3,4,5,6-pentafluorophenyl))porphyrin iron(III) chloride (FeTFPP) were investigated as P450 models for the oxidation of the mono azo dyes Disperse Black 3 (DB3), Disperse Orange 3 (DO3) and Methyl Yellow (MY) (Figure 1) using various oxidants.

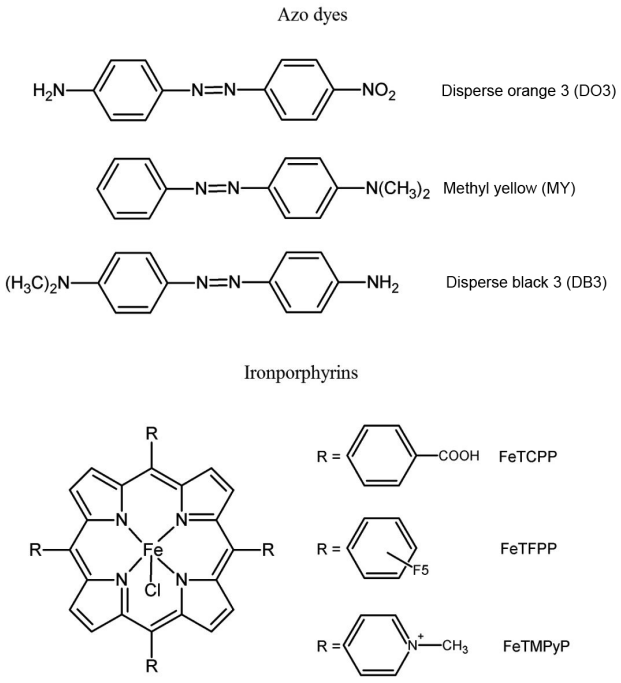

Figure 1. Structure of the dyes and catalysts used in this study.

Experimental

Materials and equipments

All the compounds used in this study were commercially available from Aldrich or Sigma and were of analytical grade purity unless otherwise stated. Hydrogen peroxide (30 wt.% solution in water) was stored at 5 °C and titrated periodically for purity assessment. *Tert*-butyl hydroperoxide (TBHP) (70 wt.% solution in water) was acquired from Acros Oganics. Iodosylbenzene (PhIO) was synthesized by hydrolysis of iodosylbenzenediacetate using a procedure adapted from the literature.[29] The solid was carefully dried under reduced pressure and kept at 5 °C; its purity was periodically controlled by iodometric titration.[30] The free base porphyrins were purchased from MidCentury. Iron insertion into the free base porphyrins was carried out using the method of Adler *et al*.[31]Acetonitrile (ACN) was HPLC grade.

UV-Vis absorption spectra were obtained on a Hewlett-Packard 8452 diode array spectrophotometer. The spectra were recorded in quartz cells with 2 mm path length (Hellma).

The gas chromatography-mass spectrometry (GC-MS) analyses were performed on a Shimadzu QP2010 mass spectrometer fitted with a GC17A gas chromatograph. The ionization voltage was 70 eV. Gas chromatography was conducted in the temperature programming mode with a DB-5MS column (30 m × 0.25 mm × 0.25 μm). The initial

column temperature was set at 50 ºC for 5 min, followed by a linear increase to 270 ºC at a rate of 10 ºC min^{-1}, and maintenance of this temperature for 4 min. The temperature of the injection port was 260 ºC, and the GC-MS interface was kept at 300 ºC. The helium carrier gas flow rate was 1.0 mL min^{-1}. The reaction products were identified by comparison of their retention times with known reference compounds, and by comparing their mass spectra to fragmentation patterns observed in the NIST spectral library stored in the computer software (version 1.10 beta, Shimadzu) of the mass spectrometer.

The high-performance liquid chromatography (HPLC) analyses were accomplished on a Shimadzu liquid chromatograph equipped with an LC-10AS solvent pump, an SPD-M 10A VP spectrophotometric detector coupled to a CTO-10A VP column oven and an SCL-10A VP system controller. The products were analyzed by using a Lichrospher 100RP-18 column with a particle size of 5 μm (125 mm × 4 mm), supplied by Merck. The analytical column was protected by a Lichrospher pre-column (4 mm × 4 mm). The mobile phase consisted of a mixture of ultrapure water (A) and acetonitrile (B). The analysis started with 30% of eluent A for 5 min, and then the concentration of the latter was increased linearly up to 70% in the following 6 min. This composition was held for further 4 min before being returned to 30% of eluent A for 2 min, to give a total run time of 22 min. The flow rate was 1.0 mL min^{-1}, the detection was carried out at 320 nm, and the column temperature was maintained at 32 ºC.

The HPLC-MS/MS analyses were performed on a Shimadzu LC-20A HPLC apparatus equipped with a diode array detector (CBM20A, Shimadzu, Kyoto, Japan) coupled to an UltrOTOFq (Bruker Daltonics, Billerica, MA, USA), ESI-qTOF (electrospray ionization-quadrupole time-of-flight) mass spectrometer operating in the positive ionization mode.

Oxidation reactions

Reactions were carried out in a 3 mL vial covered with a screw cap. A solution of disperse dye in ACN (1.25 μmol) and the oxidant (7.5 μmol) was added to the vial containing one of the ironporphyrins (0.125 μmol) in ACN/H_2O 2:1 (2 mL). This catalyst/dye/oxidant molar ratio (1:10:60) was the optimized condition to obtain higher product yields. All used ironporphyrins are soluble in the solvent mixture ACN/H_2O 2:1. Reactions were accomplished under magnetic stirring, at room temperature, for 4 h. At the end of the reaction, magnetic stirring was interrupted, and an aliquot of the reaction was analyzed by HPLC and GC-MS. The oxidation products were identified by comparing their retention times with those of authentic standards. Conversion yields were calculated on the basis of the added dyes and were determined by means of a calibration curve. Other products were identified by mass spectrometry. The oxidation percentage was computed with the aid of the UV-Vis spectroscopy and calculated on the basis of the difference between the final and initial absorbance values at the maximum absorption wavelength of the dye.

Control reactions were conducted in all the different conditions, in the absence of the ironporphyrins (blank reactions). Results confirmed that no products from dye oxidation were obtained in these conditions.

Results and Discussion

Dye oxidation monitored by UV-Vis spectroscopy

The complexes investigated as catalysts for the oxidation of DO3, DB3 and MY dyes were the commercial ironporphyrins FeTCPP, FeTFPP and FeTMPyP (Figure 1), which have been reported to be good catalysts for the oxidation of hydrocarbons, drugs and other organic molecules.[20,31-33] The reactions were carried out in ACN/H_2O (2:1, v:v), taking the solubility of the dyes and the catalysts into account.

The oxidation reactions were followed by UV-Vis spectroscopy, by monitoring the main absorption band of the DB3 (λ_{max} at 420 nm), DO3 (λ_{max} at 430 nm) and MY (λ_{max} at 410 nm) dyes, which is due to the $n \rightarrow \pi^*$ transition and is known as the azo band. The other less intense bands observed in the UV region are assigned to the electronic $\pi \rightarrow \pi^*$ transition of the aromatic ring.[9,34,35] The UV-Vis spectra of azo dyes are a "finger print" of these compounds, changes in these spectra indicate alterations in the structure of these molecules.

Figure 2 depicts the catalytic results obtained for the reactions using TBHP as oxidant and different ironporphyrins. Although FeTFPP is considered a good catalyst for the oxidation of various substrates,[31,33,36] it was not able to promote the oxidation of the studied dyes. On the other hand, the ironporphyrins bearing ionic groups, FeTMPyP and FeTCPP, virtually promoted complete disappearance of the main absorption band, indicating almost 100% dye conversion. This high conversion was also observed by us in a previous work, which used FeTMPyP supported on montmorillonite as the catalyst and the same products were observed in both systems.[20] These results reveal that ionic substituents on the porphyrin ring have important effects on the catalysis of these dyes and confirm previous observations reported for other substrates, i.e., the cooperative effects of the π-π and electrostatic interactions

between the catalyst and the substrate probably favor the oxygen transfer from the active species to the substrate.[37]

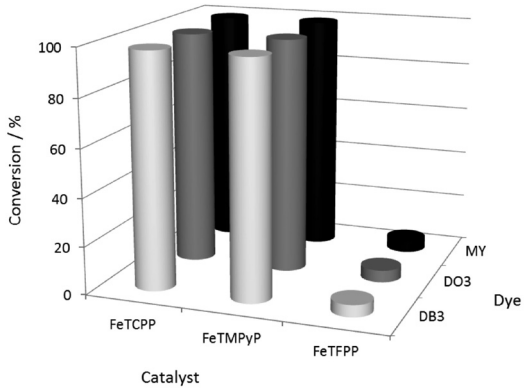

Figure 2. Conversion percentages for the dye oxidation reactions by TBHP in the presence of the ironporphyrins, as monitored by UV-Vis spectroscopy at λ of the maximum absorption band for each dye. Standard conditions as defined in the text.

Other oxidants were also evaluated, namely PhIO and H_2O_2 (Figure 3). As a simple oxygen donor, PhIO favors the formation of the high-valent oxoferryl porphyrin π-cation radical, $^{\bullet+}PFe^{IV}=O$, as the catalytic species,[19,38] responsible for the relatively high dye conversions (Figure 3). Although H_2O_2 is an environmentally clean oxidant, it leads to low conversion yields (Figure 3). This is probably due to the decomposition of this oxidant catalyzed by the metalloporphyrin which occurs in a similar way to the reaction catalyzed by the enzyme catalase,[39,40] previously verified for other similar catalytic systems involving this oxidant.[24]

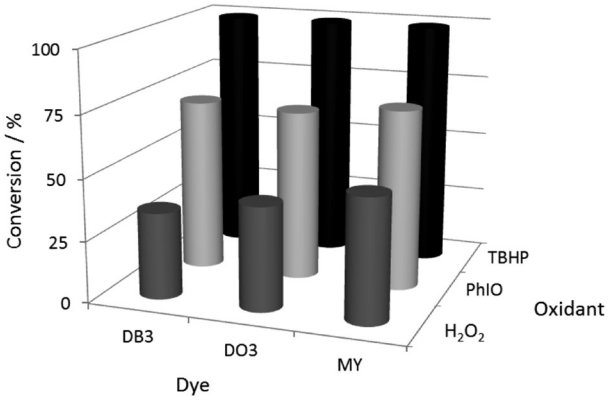

Figure 3. Conversion percentages for the dye oxidation reactions by different oxidants in the presence of FeTMPyP, as monitored by UV-vis spectroscopy at λ of the maximum absorption band for each dye. Standard conditions as defined in the text.

When alkyl peroxides such as TBHP are employed as an oxidant, the heterolytic cleavage of the O–O bond is expected to occur upon peroxide coordination to the metalloporphyrin central metal ion, giving rise to the active species oxoferryl porphyrin π-cation radical, $^{\bullet+}PFe^{IV}=O$ (Figure 4a). However, the major problem regarding the use of ROOH with ironporphyrins is the avoidance of the thermodynamically favored homolysis of the peroxide bond. Homolytic O–O bond cleavage generates a less reactive intermediate, PFe^{IV}–OH, and culminates in an alkoxyl radical $RO^{\bullet}$, which is able to abstract a hydrogen atom from a saturated C–H bond but is unable to produce epoxides from an olefinic substrate (Figure 4b).[41] The relatively high conversion yields achieved in the reactions using TBHP suggest that the heterolytic cleavage of the O–O bond takes place during the oxidation of these dyes (Figure 3).

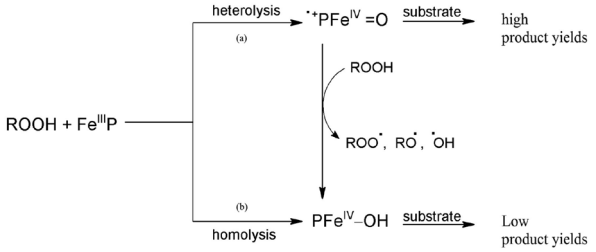

Figure 4. Possible pathway for the reactions of FeP with peroxides (adapted from reference 42).

Besides the disappearance of the azo band, the UV-Vis spectrum of the reaction medium relative to the catalytic system FeTMPyP/TBHP displayed a new absorption band at ca. 330 nm (Figure 5). In order to identify the oxidation products responsible for this absorption, the reaction mixtures were analyzed by HPLC and GC-MS. The relative product yields were determined on the basis of the calibration curves constructed by using the dye standards.

Table 1 lists the retention times obtained from the HPLC and GC-MS analyses of each dye standard as well as those verified for the oxidation products present in the reaction mixtures when the FeTMPyP/TBHP catalytic system was employed. The molecular ion and the fragmentation profiles detected during the GC-MS analysis allowed the identification of the eluted products by comparison with the mass spectra of the NIST library, with over 95% similarity (Table 1).

As for the oxidation of MY, the products 4-methylamino-azobenzene (main product, relative yield of 56%), 4-aminoazobenzene (relative yield of 26%), resulting from the mono- and bis-demethylation of the terminal amine, respectively, and 4-nitroazobenzene (relative yield of 14%), a result of the additional oxidation of the demethylated amine (Table 1), were identified. These products are in agreement with those expected from the

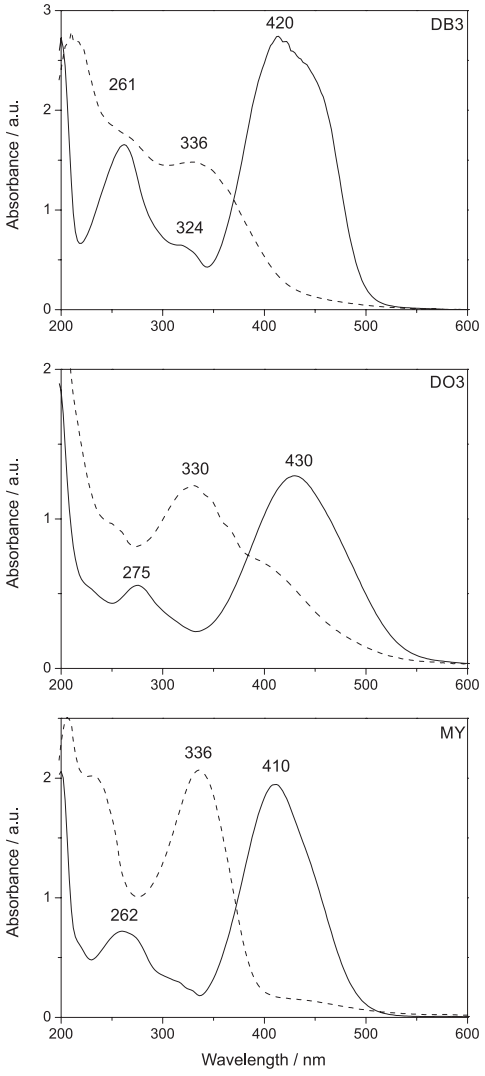

Figure 5. UV-Vis spectra of the ACN/H_2O (2:1, v:v) solutions of the DB3, DO3 and MY azo dyes (0.625 mmol L^{-1}) in the presence of FeTMPyP (0.125 μmol) before (**—**) and after (**---**) addition of 7.5 μmol TBHP.

oxidation of tertiary amines catalyzed by P450 enzymes.[11,21] Therefore, these catalytic systems can be considered good biomimetical models of P450 enzymes for MY oxidation.

Concerning DO3 and DB3, the main oxidation product was 4,4'-dinitroazobenzene, originated from the oxidation of the terminal amine in the same way that the reaction occurred in the case of MY and in accordance with what is observed for *in vivo* systems catalyzed by P450. These results indicate that similar intermediate species are probably responsible for the *in vivo* oxidation, and that in these biomimetical systems, the high-valent oxoferryl porphyrin π-cation radical, $^{\bullet+}PFe^{IV}=O$,[41,42] operates. This highly electrophylic species is able to transfer the oxygen atom to the di-amine, furnishing hydroxylamine. The latter is easily oxidized to the nitro compound, as already reported by Porta *et al.*[43] for the oxidation of aromatic amines catalyzed by ironporphyrins.

For the DO3 dye, the product 4-nitroaniline was attained (Table 1, entry 6). This compound had also been observed during the *in vitro* oxidation of this dye catalyzed by lignolytic enzymes/H_2O_2 for the fungus *Pleurotus ostreatus*.[44,45]

Reactions carried out in the absence of oxygen (argon atmosphere) gave similar results as compared to the ones conducted in air atmosphere. This attested the absence of radical mechanisms stemming from the homolytic cleavage of the peroxide O–O bond in these oxidations[41,46] and confirmed that the heterolytic cleavage was predominant in these conditions.

The fact that the high product yields obtained from the oxidation of the terminal amine groups while the azo bond was left intact evidences that the reduction in the azo absorption band in the UV-Vis spectra of these compounds may not be associated with the azo bond cleavage, but that it

Table 1. Retention times (t_R) of the compounds present in the reaction mixture obtained from the GC-MS and HPLC analyses of the oxidation of the dyes by TBHP in ACN/H_2O (2:1, v:v); molecular ion and product fragments (*m/z*) obtained from the GC-MS of the same solutions

entry	Compound (conversion / %)	t_R / min		Molecular ion / MI	Fragments, *m/z* (relative percentage)
		HPLC	CG-MS		
1	DB3	11.0	30.1	240	240 (100), 148 (10), 120 (89), 105 (14), 92 (46), 77 (17), 65 (23), 42 (58)
2	P1	10.0	–	–	nd
3	P2	10.3	–	–	nd
4	4,4'-dinitroazobenzene (82%)	10.8	28.6	272	227 (25), 150 (77), 122 (100), 92 (27), 76 (56), 50 (22)
5	P4	11.3	–	–	nd
6	DO3	12.6	29.0	242	242 (20), 212 (22), 120 (35), 92 (100), 65 (51)
7	4-nitroaniline (17%)	3.6	19.3	138	138 (75), 122 (12), 108 (67), 92 (41), 80 (21), 65 (100)
8	4,4'-dinitroazobenzene (79%)	10.8	28.4	272	272 (22), 150 (68), 122 (100), 92 (50), 76 (63)
9	MY	12.4	25.7	225	225 (89), 148 (25), 120 (100), 105 (27), 91 (14), 77 (50), 42 (58)
10	4-methylamino-azobenzene (56%)	9.6	25.4	211	211 (46), 134 (30), 106 (100), 77 (57), 65 (19), 51 (17)
11	4-aminoazobenzene (26%)	10.3	24.3	197	197 (32), 120 (38), 92 (100), 77 (39), 65 (48), 51 (15)
12	4-nitroazobenzene (14%)	11.0	24.1	227	227 (20), 122 (15), 105 (35), 77 (100), 51 (23)

nd: not detected.

may be due to the oxidation of a substituent in the aromatic ring thereby causing a shift of the azo bond absorption. This was reported in the literature for other dyes.[47]

On the basis of the catalytic results obtained in our studies, our group proposes a reaction scheme that represents the oxidation of these azo dyes by TBHP in the presence of the ironporphyrins (Figure 6).

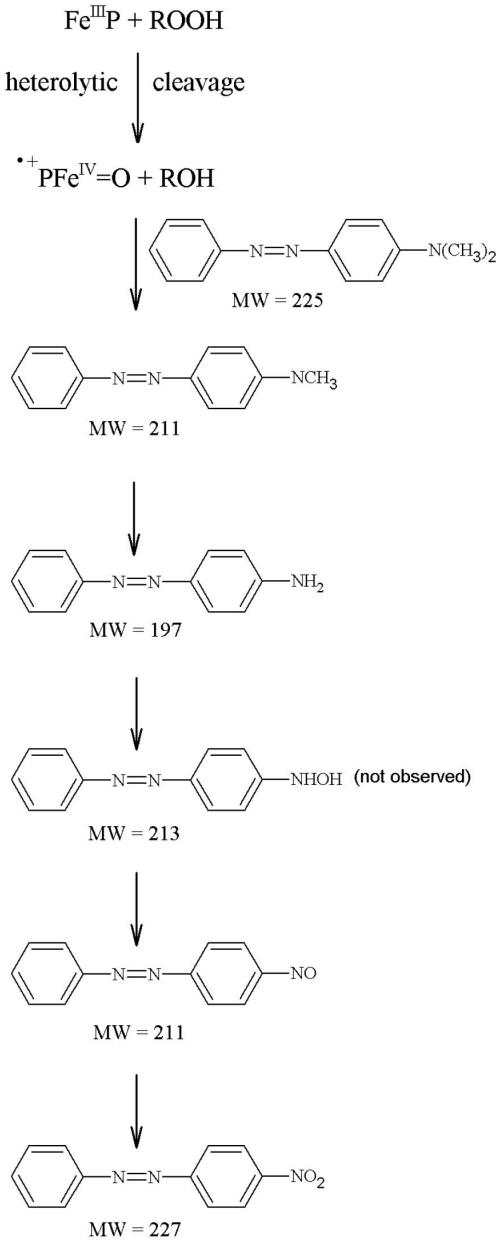

Figure 6. Proposed scheme for methyl yellow (MY) oxidation by TBHP catalyzed by FeP.

Conclusions

The investigated catalytic systems are efficient for the oxidation of azo dyes by PhIO and TBHP. The high conversion yields obtained by using PhIO indicate that the reaction goes through the mechanism involving the high-valent oxoferryl porphyrin π-cation radical, $^{\bullet+}PFe^{IV}=O$. This is probably the catalytic species that participates in the oxidation with TBHP and is formed through the heterolytic cleavage of the peroxide O–O bond. The oxidation products for all the three dyes are the result of terminal amine oxidation, while the azo bond is left intact. Similar products have been verified during DO3 oxidation in biological systems, showing that the studied catalytic systems are good biomimetical models. Therefore, the systems have potential application for evaluation of the toxicity of this class of dyes.

Supplementary Information

Supplementary information associated with this work contains HLPC and GC-MS chromatograms and mass spectra. These data are available free of charge at http://jbcs.sbq.org.br as a PDF file.

Acknowledgements

The authors thank CNPq, CAPES and FAPESP for financial support, Dr. Cynthia Maria de Campos Prado Manso for linguistic advice, Izabel Cristina C. Turatti (Faculdade de Ciências Farmacêuticas de Ribeirão Preto, USP) for the GC-MS analysis and José Carlos Tomaz (Faculdade de Ciências Farmacêuticas de Ribeirão Preto, USP) for the HPLC-MS analysis.

References

1. El-Desoky, H. S.; Ghoneim, M. M.; Zidan, N. M.; *Desalination* **2010**, *264*, 143.
2. Liu, G.; Wang, J.; Lu, H.; Jin, R.; Zhou, J.; Zhang, L.; *J. Hazard. Mater.* **2009**, *171*, 222.
3. Ayed, L.; Mahdhi, A.; Cheref, A.; Bakhrouf, A.; *Desalination* **2011**, *274*, 272.
4. Rauf, M. A.; Meetani, M. A.; Hisaindee, S.; *Desalination* **2011**, *276*, 13.
5. Wang, Y.; Bingtao, T.; Shufen, Z.; *Dyes Pigm.* **2011**, *91*, 294.
6. Crabtree, H. C.; Hart, D.; Thomas, M. C.; Witham, B. H.; McKenzie, I. G.; Smith, C. P.; *Mutat. Res. Lett.* **1991**, *264*, 155.
7. Pacheco, M. J.; Santos, V.; Ciríaco, L.; Lopes, A.; *J. Hazard. Mater.* **2011**, *186*, 1033.
8. Franciscon, E.; Piubeli, F.; Fantinatti-Garboggini, F.; de Menezes, C. R.; Silva, I. S.; Cavaco-Paulo, A.; Grossman, M. J.; Durrant, L. R; *Enzyme Microb. Technol.* **2010**, *46*, 360.
9. Saratale, R. G.; Saratale, G. D.; Chang, J. S.; Govindwar, S. P.; *J. Taiwan Inst. Chem. Eng.* **2011**, *42*, 138.

10. Platt, K. L.; Edenharder, R.; Aderhold, S.; Muckel, E.; Glatt, H.; *Mutat. Res., Genet. Toxicol. Environ. Mutagen.* **2010**, *703*, 90.
11. Hunger, K.; *Chimia* **1994**, *48*, 520.
12. Zbaida, S.; Stoddart, A. M.; Levine, W. G.; *Chem. Biol. Interact.* **1989**, *69*, 61.
13. Chen, C.-H.; Chang, C.-F.; Liu, S.-M.; *J. Hazard. Mater.* **2010**, *177*, 281.
14. Mansuy, D.; *Ann. Pharm. Fr.* **2011**, *69*, 62.
15. Hannemann, F.; Bichet, A.; Ewen, K. M.; Bernhardt, R.; *Biochim. Biophys. Acta, Gen. Subj.* **2007**, *1770*, 330.
16. Kotrbová, V.; Mrázová, B.; Moserová, M.; Martínek, V.; Hodek, P.; Hudeček, J.; Frei, E.; Stiborová, M.; *Biochem. Pharmacol.* **2011**, *82*, 669.
17. Montellano, P. R. O.; *Cytochrome P450: Structure, Mechanism and Biochemistry*, 3rd ed.; KluwerAcademic/Plenum Publishers: New York, USA, 2005.
18. Tani, F.; Matsuura, M.; Nakayama, S.; Naruta, Y.; *Coord. Chem. Rev.* **2002**, *226*, 219.
19. Mansuy, D.; *C. R. Chim.* **2007**, *10*, 392.
20. Barros, V. P.; Faria, A. L.; MacLeod, T. C. O.; Moraes, L. A. B.; Assis, M. D.; *Int. Biodeterior. Biodegrad.* **2008**, *61*, 337.
21. Emmert III, F. L.; Thomas, J.; Hon, B.; Gengenbach, A. J.; *Inorg. Chim. Acta* **2008**, *361*, 2243.
22. Zidane, Y.; Ourari, A.; Bataille, T.; Hapiot, P.; Hauchard, D.; *J. Electroanal. Chem.* **2010**, *641*, 64.
23. Biswas, A. N.; Pariyar, A.; Bose, S.; Das, P.; Bandyopadhyay, P.; *Catal. Commun.* **2010**, *11*, 1008.
24. Faria, A. L.; Mac Leod, T. O. C.; Barros, V. P.; Assis, M. D.; *J. Braz. Chem. Soc.* **2009**, *20*, 895.
25. Pálfi, T.; Wojnárovits, L.; Takács, E.; *Radiat. Phys. Chem.* **2011**, *80*, 462.
26. Hodges, G.; Smith, J. R. L.; Oakes, J.; *Stud. Surf. Sci. Catal.* **1997**, *110*, 653.
27. Serra, A. C.; Docal, C.; Gonsalves, A. M. d'A. R.; *J. Mol. Catal. A: Chem.* **2005**, *238*, 192.
28. Hager, M.; Holmberg, K.; Gonsalves, A. M. d'A. R.; Serra, A. C.; *Colloids Surf., A* **2001**, *183*, 247.
29. Saltzman, H.; Sharefkin, J. G.; *Organic Syntheses Collective*, vol. 5; John Wiley & Sons: New York, USA, 1973.
30. Lucas, H. J.; Kennedy, E. R.; *Organic Syntheses Collective*, vol. 3; John Wiley & Sons: New York, USA, 1955.
31. Zucca, P.; Rescigno, A.; Sanjust, E.; *Chin. J. Catal*. **2012**, *32*, 1663.
32. Neves, C. M. B.; Simões, M. M. Q.; Santos, I. C. M. S.; Domingues, F. M. J.; Neves, P. M. S.; Paz, F. A. A.; Silva, A. M. S.; Cavaleiro, J. A. S.; *Tetrahedron Lett*. **2011**, *52*, 2898.
33. Luz, R. C. S.; Damos, F. S.; Tanaka, A. A.; Kubota, L. T.; Gushikem, Y.; *Talanta* **2008**, *76*, 1097.
34. Zucca, P.; Sollai, F.; Garau, A.; Rescigno, A.; Sanjust, E.; *J. Mol. Catal. A: Chem.* **2009**, *306*, 89.
35. Li, J.; Jiang, P.; Wei, C.; Shi, J.; *Dyes Pigm.* **2008**, *78*, 219.
36. Rau, H.; *Azocompounds*; Elsevier: Amsterdam, 1990.
37. Mac Leod, T. C. O.; Faria, A. L.; Barros, V. P.; Queiroz, M. E. C.; Assis, M. D.; *J. Mol. Catal. A: Chem.* **2008**, *296*, 54.
38. Santos, A. C. M. A.; Smith, J. R. L.; Assis, M. D.; *J. Porphyrins Phthalocyanines* **2005**, *9*, 326.
39. Groves, J. T.; *J. Inorg. Biochem.* **2006**, *100*, 434.
40. Horst, F.; Rueda, E. H.; Ferreira, M. L.; *Enzyme Microb. Technol.* **2006**, *38*, 1005.
41. Vlasits, J.; Furtmüller, P .G.; Jakopitsch, C.; Zamocky, M.; Obinger, C.; *Biochim. Biophys. Acta, Proteins Proteomics* **2010**, *1804*, 799.
42. Nam, W.; Han, H. J.; Oh, S.-Y.; Lee, Y. J.; Choi, M.-H.; Han, S.-Y.; Kim, S.; Woo, S. K.; Shin, W.; *J. Am. Chem. Soc.* **2000**, *122*, 8677.
43. Porta, F.; Colonna, F.; Arciprete, F.; Banfi, S.; Coppa, F.; *J. Mol. Catal. A: Chem.* **1996**, *113*, 359.
44. Zhao, X.; Hardin, I. R.; *Dyes Pigm.* **2007**, *73*, 322.
45. Zhao, X.; Hardin, I. R.; Hwang, H.-M.; *Int. Biodeterior. Biodegrad.* **2006**, *57*, 1.
46. Meunier, B.; *Metal-Oxo and Metal-Peroxo Species in Catalytic Oxidations*; Springer: New York, USA, 2000.
47. Wu, T.; Lin, T.; Zhao, J.; Hidaka, H.; Serpone, H.; *Environ. Sci. Technol.* **1999**, *33*, 1379.

Submitted: December 5, 2012
Published online: May 10, 2013

FAPESP has sponsored the publication of this article.

J. Braz. Chem. Soc., Vol. 24, No. 5, S1-S4, 2013.
Printed in Brazil - ©2013 Sociedade Brasileira de Química
0103 - 5053 $6.00+0.00

Supplementary Information

Iron Porphyrins as Biomimetical Models for Disperse Azo Dye Oxidation

Valéria P. Barros* and Marilda D. Assis

Departamento de Química, Faculdade de Filosofia Ciências e Letras de Ribeirão Preto, Universidade de São Paulo, Av. Bandeirantes 3900, 14040-901 Ribeirão Preto-SP, Brazil

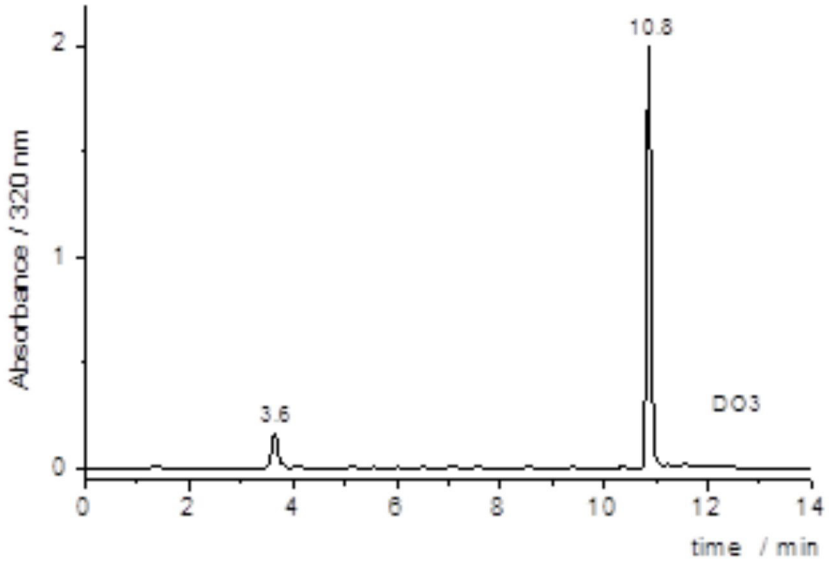

Figure S1. HPLC chromatogram of the azo dye DO3 oxidation reaction with TBHP catalyzed by FeTMPyP.

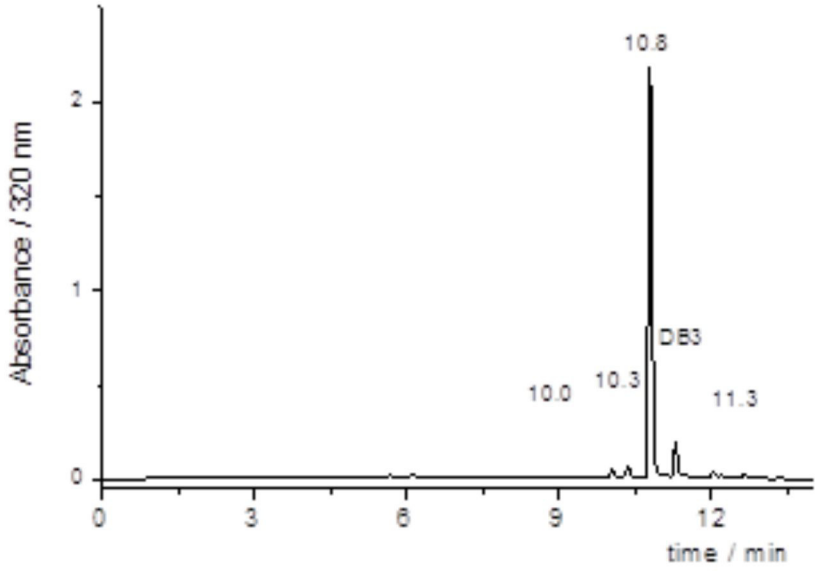

Figure S2. HPLC chromatogram of the azo dye DB3 oxidation reaction with TBHP catalyzed by FeTMPyP.

*e-mail: vpbarros@yahoo.com

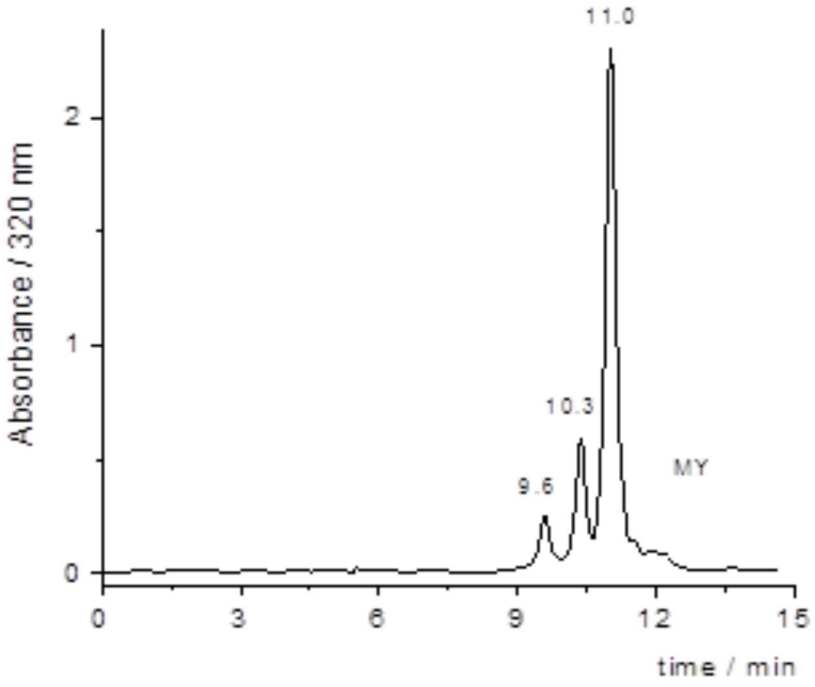

Figure S3. HPLC chromatogram of the azo dye MY oxidation reaction with TBHP catalyzed by FeTMPyP.

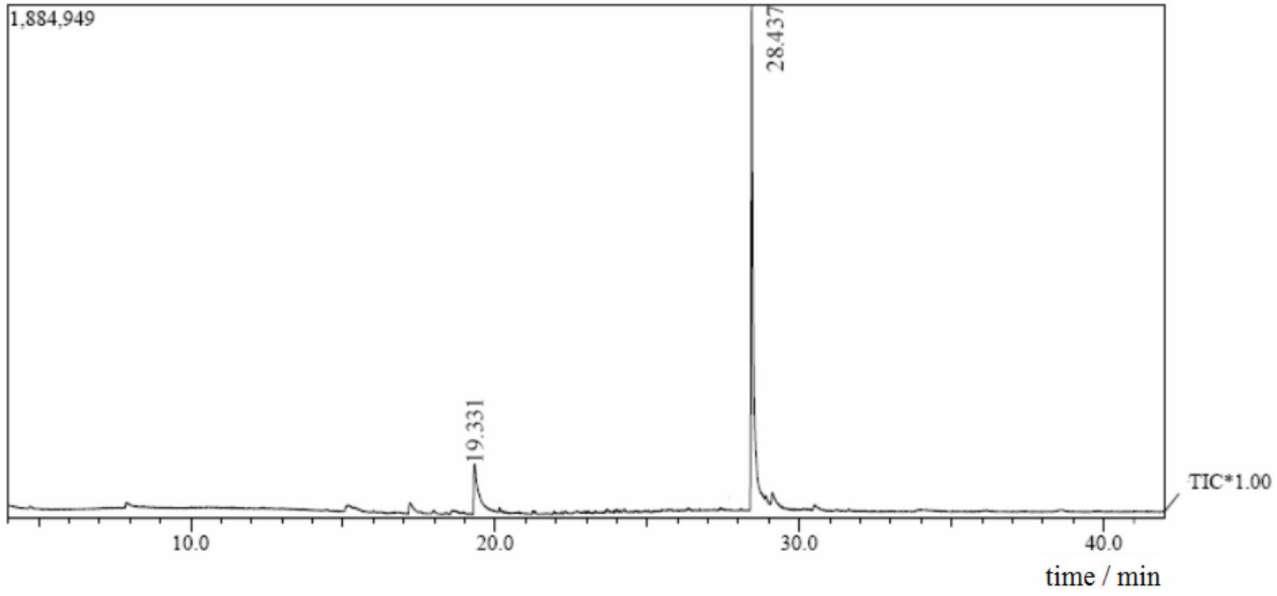

Figure S4. GC-MS chromatogram of the azo dye DO3 oxidation reaction with TBHP catalyzed by FeTMPyP.

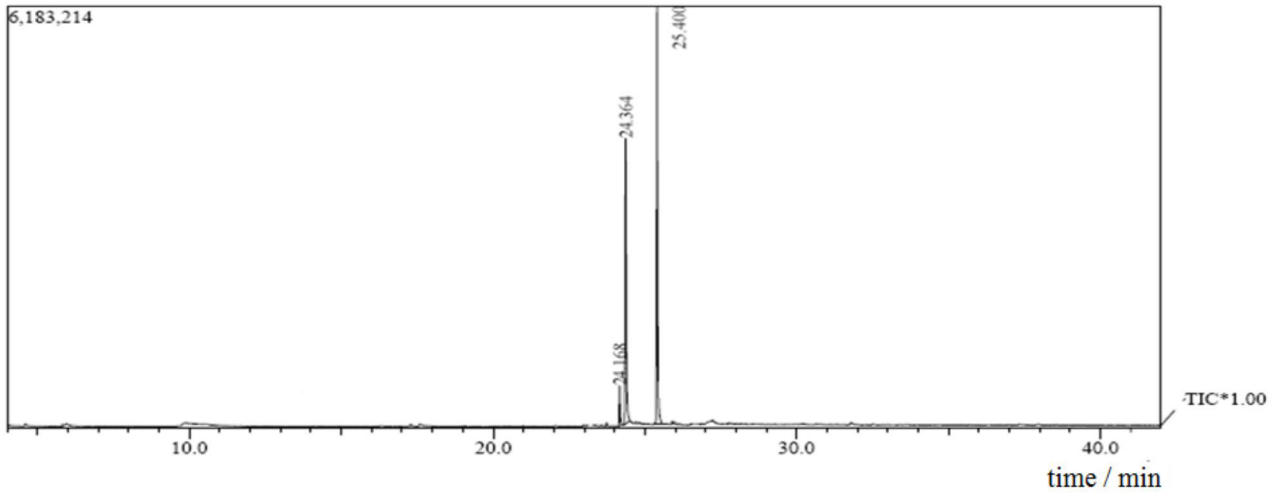

Figure S5. GC-MS chromatogram of the azo dye DB3 oxidation reaction with TBHP catalyzed by FeTMPyP.

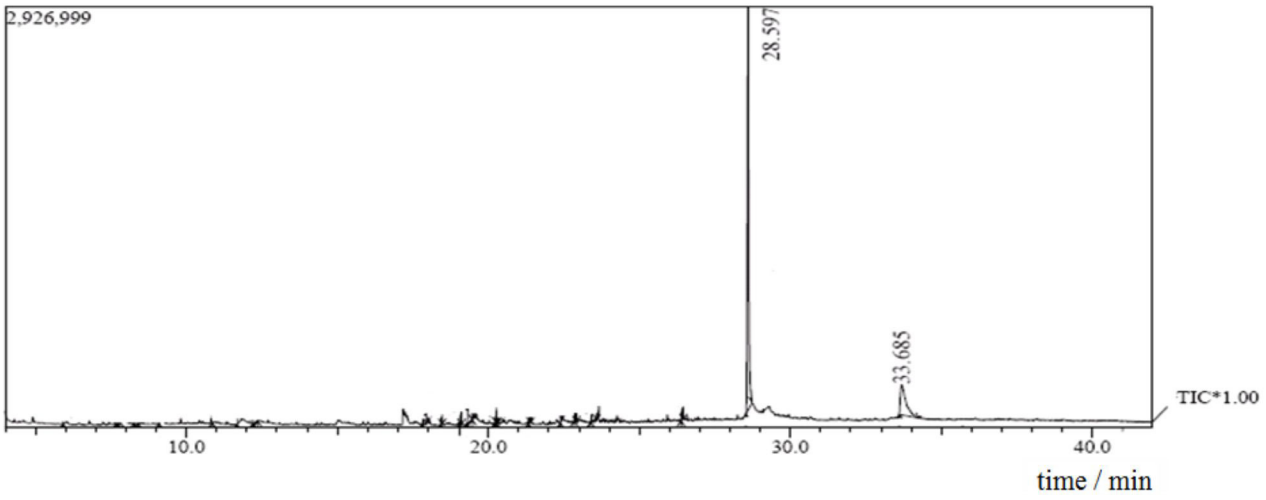

Figure S6. GC-MS chromatogram of the azo dye MY oxidation reaction with TBHP catalyzed by FeTMPyP.

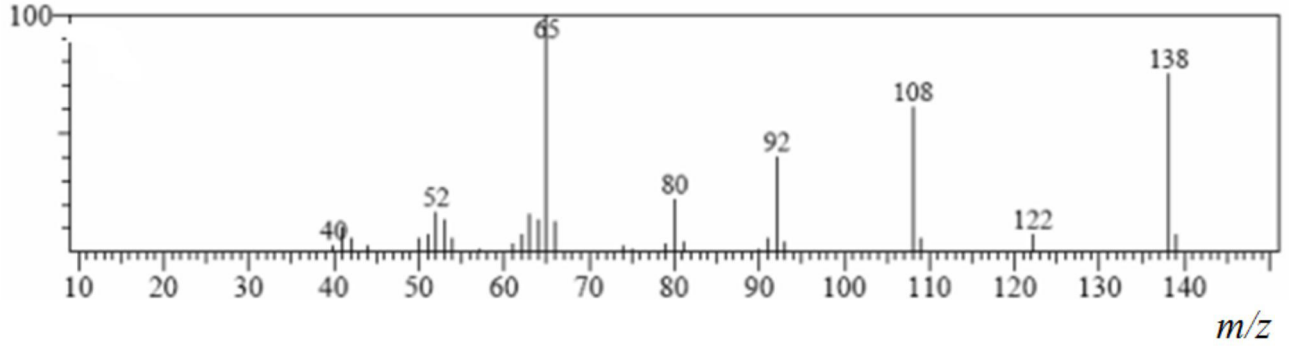

Figure S7. Mass spectrum of 4-nitroaniline.

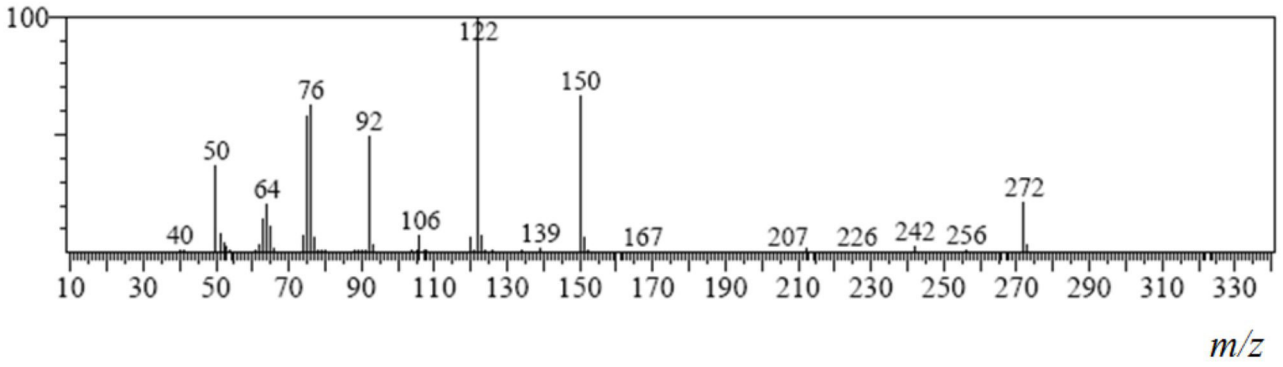

Figure S8. Mass spectrum of 4,4'-dinitroazobenzene.

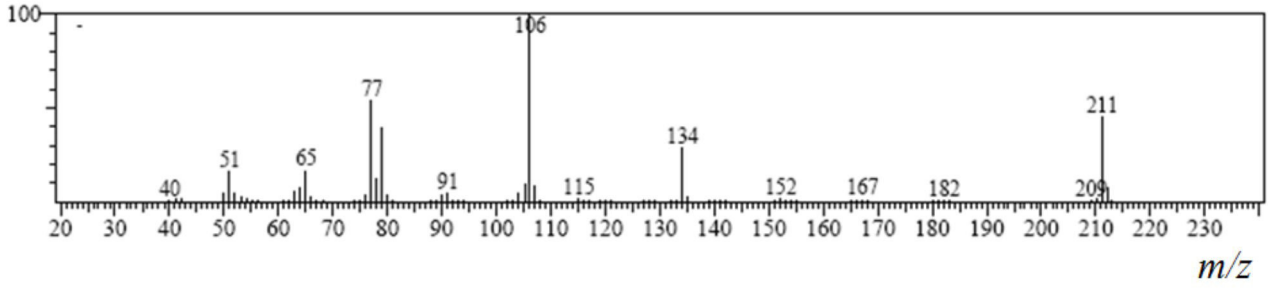

Figure S9. Mass spectrum of 4-methylamino-azobenzene.

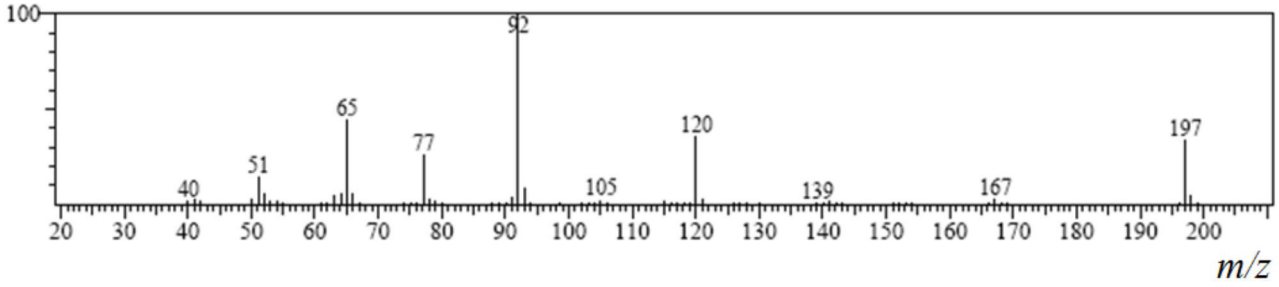

Figure S10. Mass spectrum of 4-aminoazobenzene.

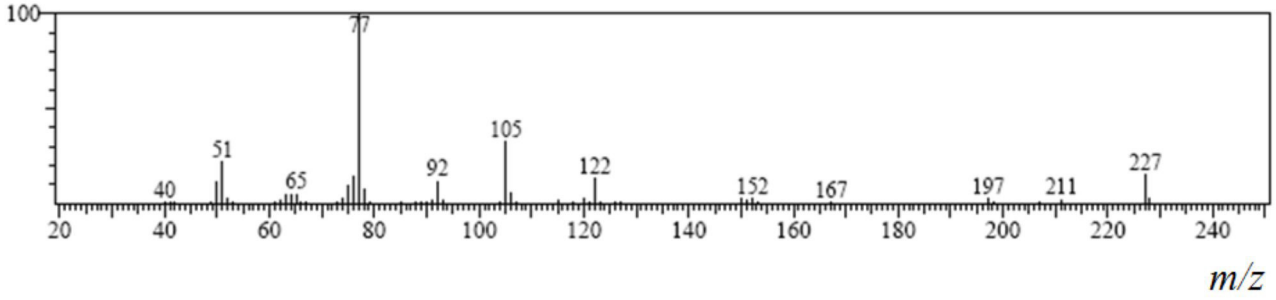

Figure S11. Mass spectrum of 4-nitroazobenzene.